ChemComm

Accepted Manuscript

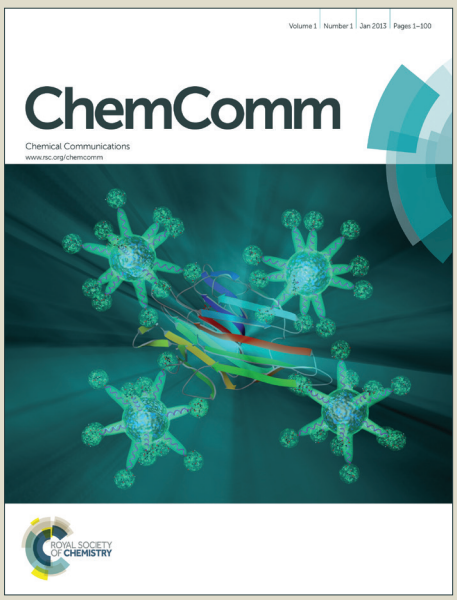

ROYAL SOCIETY OF CHEMISTRY

www.rsc.org/chemcomm

Chemical Communications

RSCPublishing

COMMUNICATION

Solvent and Electrolyte Effects on Ni($P^R_2N^{R'}_2$)$_2$-Catalyzed Electrochemical Oxidation of Hydrogen

Cite this: DOI: 10.1039/xoxxoooooox

Received ooth January 2012,
Accepted ooth January 2012

DOI: 10.1039/xoxxoooooox

www.rsc.org/

Ryan M. Stolley, Jonathan M. Darmon and Monte L. Helm*

Center for Molecular Electrocatalysis, Physical Sciences Division, Pacific Northwest National Laboratory, P.O. Box 999, K2-57, Richland, WA 99352 USA.

E-mail: monte.helm@pnnl.gov; Tel: +01-509-375-2331

Electronic Supplementary Information (ESI) available: Complete experimental details, cyclic voltammograms and electrochemical data. See DOI: 10.1039/c000000x/

We report solvent and electrolyte effects on the electrocatalytic oxidation of H_2 using Ni($P^{Cy}_2N^{R'}_2$)$_2$ (R = Bn, ^{t}Bu) complexes. A turnover frequency of 46 s^{-1} for Ni($P^{Cy}_2N^{Bn}_2$)$_2$ was obtained using 0.2 M [^{n}Bu$_4$N][BF$_4$] in THF. A turnover frequency of 51 s^{-1} was observed for Ni($P^{Cy}_2N^{tBu}_2$)$_2$ using 0.2 M [^{n}Bu$_4$N][B(C$_6$F$_5$)$_4$] in fluorobenzene. These observations, in conjunction with previous studies, indicate nitrile binding inhibits catalysis supported by Ni($P^{Cy}_2N^{Bn}_2$)$_2$.

A current goal of chemists is the selective and efficient catalytic conversion of small molecules such as H_2, O_2, N_2 and CO_2, specifically for their use in energy applications.[1-6] Considerable progress has been made toward this objective, including the use of transition metal complexes for catalytic transformations.[5,7-13] In order to improve homogeneous catalysts, identification of factors that contribute to the overall observed rate is critical for implementing rational design modifications. Most transition metal mediated molecular catalysts have a single step in common, the binding of a reactant to the metal center, which leads to bond activation and subsequent transformations. While any step in the catalytic cycle can be rate determining, substrate binding typically requires an open coordination site on the transition metal center, making this process particularly susceptible to inhibition by solvents and other reagents. Understanding the limiting factors that slow catalysis during the substrate-binding step is important for the design of improved catalysts.

The electrocatalytic oxidation of H_2 by [Ni($P^{Cy}_2N^{R'}_2$)$_2$]$^{2+}$ (e.g. R' = Bn, $(CH_2)_2OMe$, ^{t}Bu) complexes in nitrile solvents (i.e. CH_3CN, PhCN) has been extensively studied.[14-17] The mechanism of H_2 oxidation (Fig. 1) consists of addition and heterolytic cleavage of H_2 followed by alternating proton transfer (PT) and electron transfer (ET) steps. Recent experimental and computational studies from our laboratories have indicated the largest barriers that contribute to limiting catalytic activity are the H_2 addition and cleavage steps, as well as the first intermolecular deprotonation.[18-20] In particular, the calculated barrier for H_2 addition and heterolytic cleavage of the computationally studied [Ni($P^{Cy}_2N^{Me}_2$)$_2$(CH_3CN)]$^{2+}$ complex is ≈ 14 kcal/mol and the barrier for the first intermolecular deprotonation by an aniline base is estimated to be ≈ 17 kcal/mol.[15,20] A very recent report from our laboratories estimates the CH_3CN binding energy to [Ni($P^{Ph}_2N^{Ph}_2$)$_2$]$^{2+}$ to be ≈ 2 kcal/mol with a free energy dissociation barrier of ≈ 6 kcal/mol.[21] These barriers represent significant opportunities to improve rates through rational catalyst design and optimization of reaction conditions. Herein, we report the

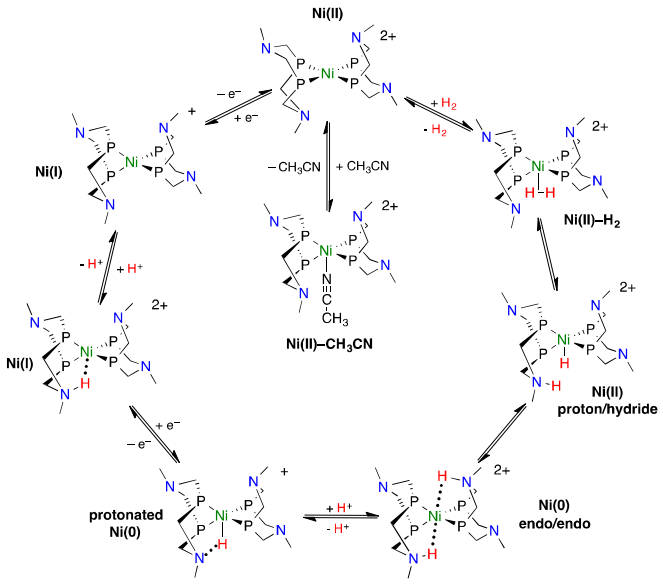

Figure 1. Proposed catalytic cycle for the oxidation of H_2 (clockwise) by [Ni($P^R_2N^{R'}_2$)$_2$]$^{2+}$ complexes.

Table 1. $Ni^{II/I}$ and $Ni^{I/0}$ $E_{1/2}$ and ΔE_p for $Ni(P^{Cy}_2N^{Bn}_2)_2$ and $Ni(P^{Cy}_2N^{Bn}_2)_2$ in various solvent/electrolyte combinations

		Redox Couple (ΔE_p)[a,b]					
Catalyst	**Solvent**	**$[A^-] = BF_4^-$**		**$[A^-] = PF_6^-$**		**$[A^-] = B(C_6F_5)_4^-$**	
		$Ni^{II/I}$	**$Ni^{I/0}$**	**$Ni^{II/I}$**	**$Ni^{I/0}$**	**$Ni^{II/I}$**	**$Ni^{I/0}$**
$Ni(P^{Cy}_2N^{Bn}_2)_2$	THF	-0.75 V (107 mV)	-1.21 V (106 mV)	-0.71 V (81 mV)	-1.24 V (83 mV)	-0.62 V (71 mV)	-1.33 V (69 mV)
	PhF	-0.78 V (119 mV)	-1.27 V (129 mV)	-0.74 V (101 mV)	-1.29 V (102 mV)	-0.65 V (78 mV)	-1.43 V (73 mV)
$Ni(P^{Cy}_2N^{tBu}_2)_2$	THF	-0.76 V (145 mV)	-1.29 V (103 mV)	-0.74 V (160 mV)	-1.33 V (87 mV)	-0.69 V (179 mV)	-1.44 V (74 mV)
	PhF	-0.84 V (166 mV)	-1.46 V (131 mV)	-0.66 V (167 mV)	-1.33 V (129 mV)	-0.69 V (152 mV)	-1.56 V (80 mV)

[a] Potentials are referenced to the $Cp_2Fe^{+/0}$ couple. [b] Conditions: 0.8 mM [Ni], 0.2 M [^{n}Bu$_4$N][A$^-$] solution, 250 mV/s.

electrocatalyzed oxidation of H_2 facilitated by $Ni(P^{Cy}_2N^{R'}_2)_2$ (R' = Bn, ^{t}Bu) complexes and discuss the effects of the solvent and electrolyte on the catalytic turnover frequencies (TOFs).[14,16] These two complexes possess different solvent binding affinities for coordinating solvents and have significantly different steric profiles around the proton relay. Additionally, these two catalysts exhibit a substantial difference in their activity in nitrile solvents, 10 s^{-1} compared to 58 s^{-1} for $Ni(P^{Cy}_2N^{Bn}_2)_2$ and $Ni(P^{Cy}_2N^{tBu}_2)_2$, respectively, making them ideal for studying the relative effects of solvent and anion binding on catalytic rate.[14,16]

Electrochemical studies were performed using Ni(0) solutions of the $Ni(P^{Cy}_2N^{R'}_2)_2$ (R' = Bn, ^{t}Bu) complexes. Solutions of the Ni(0) catalysts were used due to their superior solubility in the solvents studied, and to avoid the introduction of anions associated with the Ni(II) complexes. For each complex, the solvent and electrolyte were systematically varied to gain insight into both their electrochemical and electrocatalytic behavior.

Cyclic voltammograms (CVs) of 0.8 mM $Ni(P^{Cy}_2N^{R'}_2)_2$ (R = Bn, ^{t}Bu) in 0.2 M [^{n}Bu$_4$N][A$^-$] (A$^-$ = BF_4^-, PF_6^-, $B(C_6F_5)_4^-$) solutions of THF (e.g. Fig. 2 and ESI Fig. S2.b) and fluorobenzene (PhF, ESI Fig. S1.a and S2.a) were collected, and the data is reported in Table 1. For both complexes, the peak current (i_p) of the Ni(I/0) couple linearly correlates with the square root of the scan rate (ESI Fig. S3–7), indicative of a diffusion-controlled electrochemical event. The i_p values of the Ni(II/I) couple show non-linear behavior in the plots of i_p versus the square root of scan rate, particularly in the case of $Ni(P^{Cy}_2N^{tBu}_2)_2$ (ESI Fig. S6–7). The difference in the cathodic and anodic peak potentials (ΔE_p) at scan rates of 0.25 V/s^{-1} range from 69–167 mV, whereas the ΔE_p of the internal standard (either $[Cp_2Co][PF_6]$ or $[Cp^*_2Co][PF_6]$) ranges from 65 to 105 mV. This CV data, combined with previous results, indicate that less coordinating environments (i.e. RCN > THF > PhF and BF_4^- > PF_6^- > $B(C_6F_5)_4^-$) result in a decreased peak-to-peak separation (ΔE_p) with a simultaneous increase in the separation of the Ni(II/I) and Ni(I/0) peak potentials ($\Delta E_{1/2}$).[14-16] The solubility of $Ni(P^{Cy}_2N^{tBu}_2)_2$ in the Ni(II-0) oxidation states is too low in CH_3CN to allow for comparison, however, electrochemical data for $Ni(P^{Cy}_2N^{Bn}_2)_2$ is available.[14-16] Comparing the $\Delta E_{1/2}$ of the Ni(II/I) and Ni(I/0) peak potentials of $Ni(P^{Cy}_2N^{Bn}_2)_2$ from the most coordinating environment (i.e. CH_3CN, A$^-$ = BF_4^-, $\Delta E_{1/2}$ = 480 mV) to the least (i.e. PhF, A$^-$ = $B(C_6F_5)_4^-$, $\Delta E_{1/2}$ = 780 mV) results in an increase in their separation by 300 mV. This increased separation between the redox couples is consistent with a report by Geiger that attributes the difference directly to the ion-pairing ability of the electrolyte anion with the oxidized species.[22,23]

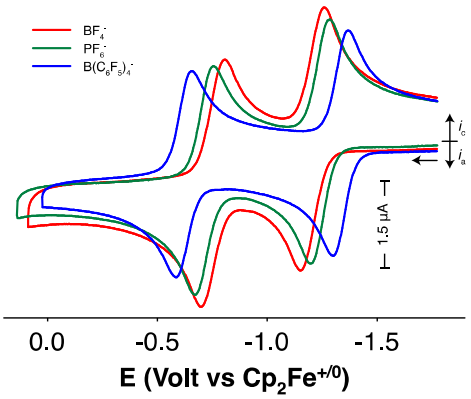

Figure 2. Cyclic voltammograms of 0.8 mM $Ni(P^{Cy}_2N^{Bn}_2)_2$ in 0.2 M [^{n}Bu$_4$N][A$^-$], A$^-$ = BF_4^- (red), PF_6^- (green), $B(C_6F_5)_4^-$ (blue) solutions of THF. Conditions: scan rate 0.250 V s^{-1} at 25 °C.

Catalytic electrochemical measurements were conducted under identical conditions at 1 atm of H_2 with subsequent additions of ^{n}BuNH$_2$ (pK_a [^{n}BuNH$_3$]$^+$ = 18.26 in CH_3CN) to remove protons.[24,25] The sterically small ^{n}BuNH$_2$ was chosen as the exogeneous base for its ability to more readily access the *endo* protons in the **Ni(0) endo/endo** isomer (Fig. 1) relative to more sterically demanding amines (i.e. NEt_3), thereby leading to greater TOFs.[16,17] An increase in the anodic peak current, i_{cat} (determined at the point where the wave first plateaus Fig. S8 in the ESI) clearly establishes catalytic H_2 oxidation (Fig. 3 and Fig. S9–14 in the ESI). The peak current for the catalytic waves, i_{cat}, as a function of scan rate was measured to determine when steady state conditions were reached; catalytic wave shapes and scan rate independent i_{cat} values were best defined at a scan rate of 0.25 V/s, with the exception of $Ni(P_2^{Cy}N_2^{Bn})_2$ in THF with A = BF_4^-, which showed steady state behavior at scan rates ≥ 0.50 V/s (ESI Fig. S12). Turnover frequencies (k_{obs}) were determined from the ratio of i_{cat}/i_p using equation 1 and reported with the corresponding half-peak potential of the catalytic wave ($E_{cat/2}$) in Table 2 (see the ESI for detailed information).[26-30] In all cases i_p values obtained from the Ni(I/0) couple were used to calculate the TOFs.

$$k_{obs} = 1.94\ V^{-1} \cdot \upsilon \left(\frac{i_{cat}}{i_p}\right)^2 \quad (1)$$

The TOF and $E_{cat/2}$ values shown in Table 2 were analyzed as a function of the coordinating ability of the solvent and electrolyte anion, and compared to previously reported studies in nitrile solvents. For reference, nitrile solutions with BF_4^- anion represent the most coordinating environment, whereas fluorobenzene solutions of $[^nBu_4N][B(C_6F_5)_4]$ represent the least coordinating environment.

The $E_{cat/2}$ values shifted to more positive values when moving to less coordinating environments. Specifically, $E_{cat/2}$ for both $Ni(P^{Cy}_2N^{Bn}_2)_2$ and $Ni(P^{Cy}_2N^{tBu}_2)_2$ shift to more oxidizing potentials by ≥ 300 mV. This positive shift in oxidation potential is likely a result of the decreased stabilization of the oxidized species in the less coordinating environments.[22,23] One notable outlier in this trend is the $E_{cat/2}$ observed for $Ni(P^{Cy}_2N^{tBu}_2)_2$ in PhF/$[^nBu_4N][B(C_6F_5)_4]$, which

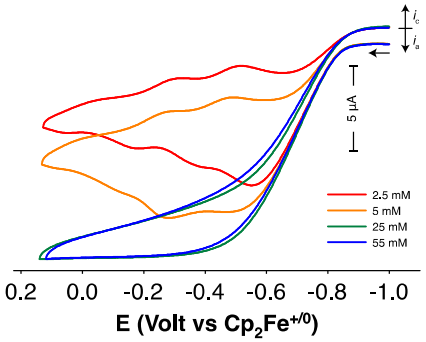

Figure 3. Cyclic voltammograms of 0.8 mM $Ni(P^{Cy}_2N^{Bn}_2)_2$ in 0.2 M $[^nBu_4N][BF_4]$ in PhF with subsequent additions of $^nBuNH_2$. Conditions: scan rate 0.250 V s^{-1} at 25 °C.

occurs 820 mV more positive than in PhCN. This large shift in catalytic potential is indicative of a change in the catalytic mechanism from the deprotonation/oxidation mechanism (PT-ET) shown in Figure 1, to an oxidation/deprotonation mechanism (ET-PT) as previously observed.[16,17] This suggests that the rate of deprotonation of the **Ni(0) endo/endo** species under these conditions is significantly hindered, resulting in the mechanistic change. These combined data clearly illustrate that the potential at which catalysis occurs and the mechanism are highly sensitive to the coordinating ability of the environment.

In $[Ni(P^R_2N^{R'}_2)_2]^{2+}$ complexes, the binding affinity for a fifth ligand (e.g. solvent) depends on the tetrahedral distortion around the nickel center and the electron donating ability of the substituents on the P and N atoms.[21,31] The $Ni(P^{Cy}_2N^{Bn}_2)_2$ complex is more susceptible to nitrile binding upon oxidation to Ni(II) compared to $Ni(P^{Cy}_2N^{tBu}_2)_2$ and the TOF data in less-coordinating environments supports this conclusion. In the case of $Ni(P^{Cy}_2N^{Bn}_2)_2$, the TOF in MeCN (15 s^{-1}) was significantly enhanced in less-coordinating environments (28–42 s^{-1}). The same trend is not observed for $Ni(P^{Cy}_2N^{tBu}_2)_2$ (with an exception in PhF/$[^nBu_4N][B(C_6F_5)_4]$, where a different mechanism is operating).[16,17] The calculated TOF of $Ni(P^{Cy}_2N^{tBu}_2)_2$ in PhCN using the Ni(I/0) couple for the i_p value was found to be 38 s^{-1} compared to less-coordinating solvents with observed TOFs of 29–38 s^{-1} (Table 2). In the absence of solvent binding, which inhibits catalysis with $Ni(P^{Cy}_2N^{Bn}_2)_2$, the TOFs often exceed those observed for $Ni(P^{Cy}_2N^{tBu}_2)_2$ under identical conditions. This observed trend in TOFs in less-coordinating solvents indicates that formation of the **Ni(II)-H_2** adduct is a contributing factor to the overall observed rates.

Table 2. Turnover frequencies (s^{-1}) as a function of solvent/supporting electrolyte combination.

Catalyst	Solvent	$[A^-] = BF_4^-$	$[A^-] = PF_6^-$	$[A^-] = B(C_6F_5)_4^-$
			TOF_{max} ^{a,b} ($E_{cat/2}$) ^{c}	
$Ni(P^{Cy}_2N^{Bn}_2)_2$	MeCN	15 s^{-1} (-0.73 V)	-	-
	PhCN ^{d}	-	22 s^{-1} (-0.68 V)	-
	THF	42 s^{-1} ^{e} (-0.69 V)	41 s^{-1} (-0.66 V)	28 s^{-1} (-0.53 V)
	PhF	38 s^{-1} (-0.69 V)	40 s^{-1} (-0.65 V)	28 s^{-1} (-0.42 V)
$Ni(P^{Cy}_2N^{tBu}_2)_2$	PhCN	-	38 s^{-1} ^{f} -0.77 V	-
	THF	38 s^{-1} (-0.67 V)	35 s^{-1} (-0.58 V)	33 s^{-1} (-0.47 V)
	PhF	29 s^{-1} (-0.65 V)	33 s^{-1} (-0.54 V)	51 s^{-1} (+0.05 V)

^{a}Conditions: 0.8 mM [Ni], 40-60 mM $^nBuNH_2$, 0.2 M $[Bu_4N^+][A^-]$, scan rate: 250 mV/s, glassy carbon working electrode, Cp*$CoPF_6$ as an internal standard. $^b i_p$ from $Ni^{I/0}$ couple. ^{c}Referenced to Fc^+/Fc couple. ^{d}[Ni] = $[Ni(P_2^{Cy}N_2^{Bn})_2](BF_4)_2$. ^{e}A TOF_{max} of 46 s^{-1} was calculated at 500 mV/s. ^{f}Calculated from original reported data using i_p from $Ni^{I/0}$.[15,16]

Surprisingly, higher TOFs were observed for $Ni(P^{Cy}_2N^{Bn}_2)_2$ compared to $Ni(P^{Cy}_2N^{tBu}_2)_2$ in non-nitrile solvents in nearly all cases. The differences are likely due to the steric environment around the pendant amine and the resulting effect on intermolecular deprotonation. This hypothesis is supported by the catalytic behavior of $Ni(P^{Cy}_2N^{tBu}_2)_2$ in PhF with $[^nBu_4N][B(C_6F_5)_4]$ as the supporting electrolyte. In addition to the substantial increase in $E_{cat/2}$, these conditions yielded the highest TOF observed in this study, although catalysis occurs through a different mechanism. We have previously shown that oxidation of the **Ni(0) endo/endo** species weakens the Ni•••HN hydrogen bonds, allowing facile chair/boat isomerization and subsequent deprotonation.[16,17,32,33] The combination of high TOF and shift of mechanism demonstrates strong evidence that deprotonation continues to contribute to the overall rate of catalysis and is a critical issue in mechanism of $Ni(P^{Cy}_2N^{R'}_2)_2$-catalyzed H_2-oxidation.

In conclusion, we have shown that the coordinating environment induced by the solvent and electrolyte has a significant impact the oxidation of H_2 by $Ni(P^{Cy}_2N^{R'}_2)_2$ (R = Bn, ^{t}Bu) electrocatalysts. In particular, more coordinating environments lead to stabilization of reactive intermediates resulting in lowering the potential at which electrocatalysis occurs. In contrast, binding of a solvent molecule (e.g. nitriles) can limit turnover frequencies through competitive binding during the H_2 addition steps. Work continues in our laboratories to explore and elucidate the effects of the medium on the electrocatalytic production and oxidation of H_2.

This research was supported as part of the Center for Molecular Electrocatalysis, an Energy Frontier Research Center funded by the U.S. Department of Energy, Office of Science,

Office of Basic Energy Sciences. Pacific Northwest National Laboratory is operated by Battelle for the U.S. Department of Energy.

Notes and references

1. N. S. Lewis and D. G. Nocera, *Proc. Natl. Acad. Sci. U.S.A.*, 2006, **103**, 15729–15735.
2. M. Winter and R. J. Brodd, *Chem. Rev.*, 2004, **104**, 4245–4270.
3. E. I. Solomon, P. Chen, M. Metz, S. K. Lee, and A. E. Palmer, *Angew. Chem., Int. Ed.*, 2001, **40**, 4570–4590.
4. Y. Tanabe and Y. Nishibayashi, *Coord. Chem. Rev.*, 2013, **257**, 2551–2564.
5. A. M. Appel, J. E. Bercaw, A. B. Bocarsly, H. Dobbek, D. L. DuBois, M. Dupuis, J. G. Ferry, E. Fujita, R. Hille, P. J. A. Kenis, C. A. Kerfeld, R. H. Morris, C. H. F. Peden, A. R. Portis, S. W. Ragsdale, T. B. Rauchfuss, J. N. H. Reek, L. C. Seefeldt, R. K. Thauer, and G. L. Waldrop, *Chem. Rev.*, 2013, **113**, 6621–6658.
6. U. Eberle, M. Felderhoff, and F. Schüth, *Angew. Chem., Int. Ed.*, 2009, **48**, 6608–6630.
7. R. M. Bullock, A. M. Appel, and M. L. Helm, *Chem. Commun.*, 2014, DOI:10.1039.C3CC46135A.
8. W. J. Shaw, M. L. Helm, and D. L. DuBois, *Biochim. Biophys. Acta, Bioenerg.*, 2013, **1827**, 1123–1139.
9. Y. Sun, J. P. Bigi, N. A. Piro, M. L. Tang, J. R. Long, and C. J. Chang, *J. Am. Chem. Soc.*, 2011, **133**, 9212–9215.
10. P. Du and R. Eisenberg, *Energy Environ. Sci.*, 2012, **5**, 6012–6021.
11. C. T. Carver, B. D. Matson, and J. M. Mayer, *J. Am. Chem. Soc.*, 2012, **134**, 5444–5447.
12. B. A. MacKay and M. D. Fryzuk, *Chem. Rev.*, 2004, **104**, 385–402.
13. S. Hinrichsen, H. Broda, C. Gradert, L. Söncksen, and F. Tuczek, *Annu. Rep. Prog. Chem., Sect. A: Inorg. Chem.*, 2012, **108**, 17–47.
14. A. D. Wilson, R. H. Newell, M. J. McNevin, J. T. Muckerman, M. Rakowski DuBois, and D. L. DuBois, *J. Am. Chem. Soc.*, 2006, **128**, 358–366.
15. J. Y. Yang, S. Chen, W. G. Dougherty, W. S. Kassel, R. M. Bullock, D. L. DuBois, S. Raugei, R. J. Rousseau, M. Dupuis, and M. Rakowski DuBois, *Chem. Commun.*, 2010, **46**, 8618–8620.
16. J. Y. Yang, S. E. Smith, T. Liu, W. G. Dougherty, W. A. Hoffert, W. S. Kassel, M. Rakowski DuBois, D. L. DuBois, and R. M. Bullock, *J. Am. Chem. Soc.*, 2013, **135**, 9700–9712.
17. P. Das, M.-H. Ho, M. J. O'Hagan, W. J. Shaw, R. M. Bullock, S. Raugei, and M. L. Helm, *Dalton Trans.*, 2014, **43**, 2744–2754.
18. M. J. O'Hagan, W. J. Shaw, S. Raugei, S. Chen, J. Y. Yang, U. J. Kilgore, D. L. DuBois, and R. M. Bullock, *J. Am. Chem. Soc.*, 2011, **133**, 14301–14312.
19. M. J. O'Hagan, M.-H. Ho, J. Y. Yang, A. M. Appel, M. Rakowski DuBois, S. Raugei, W. J. Shaw, D. L. DuBois, and R. M. Bullock, *J. Am. Chem. Soc.*, 2012, **134**, 19409–19424.
20. S. Raugei, S. Chen, M.-H. Ho, B. Ginovska-Pangovska, R. J. Rousseau, M. Dupuis, D. L. DuBois, and R. M. Bullock, *Chem.-Eur. J.*, 2012, **18**, 6493–6506.
21. J. A. Franz, M. J. O'Hagan, M.-H. Ho, T. Liu, M. L. Helm, S. Lense, D. L. DuBois, W. J. Shaw, A. M. Appel, S. Raugei, and R. M. Bullock, *Organometallics*, 2013, **32**, 7034–7042.
22. F. Barrière and W. E. Geiger, *J. Am. Chem. Soc.*, 2006, **128**, 3980–3989.
23. W. E. Geiger and F. Barrière, *Acc. Chem. Res.*, 2010, **43**, 1030–1039.
24. I. M. Kolthoff, M. K. Chantooni, and S. Bhowmik, *Anal. Chem.*, 1967, **39**, 1627–1633.
25. K. Izutsu, *Acid-Base Dissociation Constants in Dipolar Aprotic Solvents*, Blackwell Scientific Publications, 1990.
26. R. S. Nicholson and I. Shain, *Anal. Chem.*, 1964, **36**, 706–723.
27. J. M. Savéant and E. Vianello, *Electrochim. Acta*, 1965, **10**, 905–920.
28. J. M. Savéant and E. Vianello, *Electrochim. Acta*, 1967, **12**, 629–646.
29. J. M. Savéant, *Acc. Chem. Res.*, 1980, **13**, 323–329.
30. M. P. Stewart, M.-H. Ho, S. Wiese, M. L. Lindstrom, C. E. Thogerson, S. Raugei, R. M. Bullock, and M. L. Helm, *J. Am. Chem. Soc.*, 2013, **135**, 6033–6046.
31. B. R. Galan, J. Schöffel, J. C. Linehan, C. Seu, A. M. Appel, J. A. S. Roberts, M. L. Helm, U. J. Kilgore, J. Y. Yang, D. L. DuBois, and C. P. Kubiak, *J. Am. Chem. Soc.*, 2011, **133**, 12767–12779.
32. E. S. Wiedner, J. Y. Yang, S. Chen, S. Raugei, W. G. Dougherty, W. S. Kassel, M. L. Helm, R. M. Bullock, M. Rakowski DuBois, and D. L. DuBois, *Organometallics*, 2012, **31**, 144–156.
33. S. Lense, M.-H. Ho, S. Chen, A. Jain, S. Raugei, J. C. Linehan, J. A. S. Roberts, A. M. Appel, and W. J. Shaw, *Organometallics*, 2012, **31**, 6719–6731.

